A System and Methodology for Non-Contact Measurement of a Wheel Speed: a Case Study on Cardio Machines

Marcel Luzar,
State University of Applied Sciences in Głogów, P. Skargi Street 5, 67-200 Głogów

Kacper Ostrowski, Józef Korbicz
University of Zielona Góra, Institute of Control and Computation Engineering, Podgórna Street 50, 65-246 Zielona Góra, Poland

Rafał Kasperowicz, Mateusz Semegen
Heavy Kinematic Machines Sp. z o.o., Komorowo 4, 64-200 Komorowo, Poland

Abstract: In this study, a novel approach for measuring the velocity of a wheel is proposed. The paper specifically focuses on determining wheel dimensions such as radius, diameter, or circumference in order to calculate speed. The proposed algorithm can be used where the exact dimension of the wheel is unknown or difficult to measure. This article presents the use of the proposed solution for measuring the speed of rollers that move the belt on a training treadmill. The originality of approach presented in this paper is confirmed by patent number WO2022089764A1.

Keywords: optoelectronic sensor, measurements, data acquisition

1. Introduction

Wheel speed measurement is a fundamental aspect of various engineering applications such as automotive control, robotics, and manufacturing systems [1–3]. Conventional methods for measuring wheel speed involve the use of a speed sensor in contact with the wheel, which can result in inaccurate measurements due to wear and tear of the sensor or wheel [4]. Non-contact methods have been proposed as an alternative to overcome these limitations (for example, this includes cycling computers that operate using a magnetic sensor and a magnet mounted on a wheel spoke) [5]. To determine speed, most methods require prior knowledge of the wheel dimensions, such as radius, diameter, or circumference. Such systems are inaccurate because they do not account for factors like varying tire pressures, which can lead to different circumferences while riding.

More sophisticated solutions utilize Global Positioning System (GPS) signals or similar technology to determine movement speed [6, 7]. However, GPS systems generally require a person to be outdoors and moving in space, which is not applicable for stationary devices like treadmills or indoor cycling systems.

Nowadays, there is an increasing demand for fitness equipment, such as treadmills, to be equipped with modern features and capabilities that enable their integration with smart technology [8]. These functionalities allow for the collection and analysis of workout data [9], real-time progress monitoring [10, 11], personalized training programs [12], and easier access to various multimedia and training content. As a result, users can more effectively monitor their progress and adjust their training to their individual needs and goals. The introduction of smart technology to fitness equipment has contributed to the increased popularity and effectiveness of workouts [13]. Moreover, by leveraging the power of artificial intelligence, it is now feasible to construct advanced training models that can analyse and interpret data gathered from gym equipment. These models can process a wide range of inputs, including number of repetitions, movement patterns, exercise duration, speed, distance and many others, to provide valuable insights and personalized recommendations to users. Neural networks, in particular, have proven to be highly effective in capturing complex relationships within the collected data [14, 15]. Through extensive training, these models can learn to identify patterns, detect anomalies, and make accurate predictions based on the input received. This enables them to understand individual workout routines, track progress over time, and even anticipate potential injuries or overexertion.

Even old or outdated fitness equipment can be modernized by adding appropriate accessories or equipment to them. This allows for the integration of smart technology and access to the latest features and capabilities without the need to replace the entire device. Thus, many monitoring systems are called retrofit systems. Upgrading fitness equipment in this way can be a cost-effective solution for gym owners and fitness enthusiasts who want to stay up-to-date with the latest advancements in fitness technology. Often, these legacy systems have very limited access to elements that can serve as indirect indica-

Autor korespondujący:
Marcel Luzar, m.luzar@pans.glogow.pl

Artykuł recenzowany
nadesłany 22.10.2024 r., przyjęty do druku 06.12.2024 r.

tors for calculating speed. This is because older systems may not have been designed with the latest technology or features, making it difficult to incorporate new and advanced methods of speed measurement. In addition, older systems may not have the necessary sensors or equipment to accurately measure indirect indicators of speed, such as changes in tire pressure or resistance. As a result, retrofitting such systems with newer technology or accessories may be necessary to improve their speed measurement capabilities and accuracy. For instance, on a treadmill, its movement may be linked to the rotation of a drive wheel or shaft, but accessing its dimensions – such as radius, diameter, or circumference – is challenging. This is because the dimensions of the drive wheel or shaft are not readily visible or accessible, and may require disassembly of the treadmill or specialized tools to measure. Additionally, the dimensions may vary depending on factors such as wear and tear or manufacturing variability, further complicating the measurement process. As a result, accurate speed measurement on a treadmill may require advanced methods or technologies that can account for these factors and provide more precise measurements. It would be advantageous to provide a system and method for measuring speed without prior knowledge of a wheel dimension. This would enable accurate speed measurement on legacy systems that may not have the latest technology or sensors to provide indirect speed measurement. The aim of this paper is therefore to propose such a system and method for measuring speed on legacy systems. This method would rely on innovative approaches that can accurately measure speed without requiring access to the wheel dimension or other indirect indicators. By improving speed measurement capabilities on legacy systems, this proposed method has the potential to improve the accuracy and effectiveness of workouts and other fitness activities.

In this paper, we propose a system and methodology for non-contact measurement of wheel rotational speed without prior knowledge of its dimensions. The proposed approach utilizes a novel algorithm for estimating the wheel radius based on the measurement obtained with optical sensor. The results of experiments show that the proposed method provides accurate and reliable wheel speed measurements even in the absence of prior knowledge of the wheel dimension. The proposed method can be applied to measure the speed of a treadmill belt which is driven by rollers. In this application, the proposed system can be mounted above the belt and aimed at the rollers to measure the belt speed without the need for direct contact with the belt surface. This makes the proposed system an attractive solution for fitness equipment manufacturers who are looking to integrate a reliable and accurate speed measurement system into their treadmills. Furthermore, the proposed method can be extended to other applications where the measurement of rotational speed is required without prior knowledge of the object's dimensions. Examples of such applications in industry include monitoring the speed of turbines in power plants, controlling the rotational speed of machinery in automated manufacturing processes, and measuring the performance of pumps and compressors in fluid transport systems. The novelty of approach presented in this paper is confirmed by patent number WO2022089764A1 [14]. This paper can be perceived as an extension of [9] on cardio machines.

2. Measurement algorithm

The aim of this paper is to present a novel method for measuring the rotational speed of a wheel. The suggested approach consists of determining the duration a marker remains at a specific location monitored by a sensor during two successive detections, labeled as T_1 and T_3, with the interval between

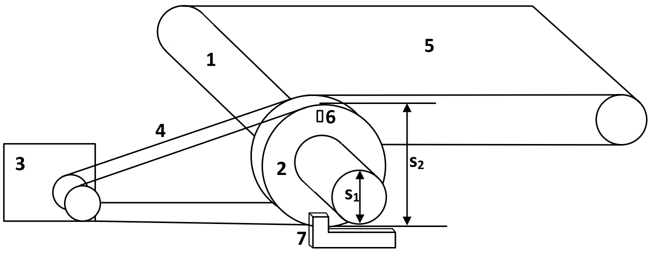

Fig. 1. A basic diagram of a standard treadmill
Rys. 1. Uproszczony schemat działania bieżni treningowej

these detections recorded as T_2. The marker, characterized by a width of Y_m and a length aligned with the radius of the wheel being measured, is utilized to determine the circumference of the circle where it is detected. The wheel's speed is subsequently calculated by using the total time required for a full rotation of the wheel (Fig. 1 – (2)) along with the measured circumference.

Figure 1 presents a basic diagram of a standard treadmill, which consists of:
1. a driving shaft with a diameter S_1,
2. a driving wheel with a diameter S_2,
3. a motor,
4. a transmission belt,
5. a working belt for user excersise.

To apply the presented method, each device needs to be equipped with an additional:
6. a light-reflective marker,
7. a sensor.

Let us introduce additional notations:
- C_m – a number of markers,
- O_{S1} – a circumference of a shaft.

The described method can also be applied to other devices, such as an exercise bike, a stair climber, or similar equipment, which generally operate using a rotating shaft and a driving wheel.

In Fig. 2 the exemplary placement of the markers are presented where:
- M_0, M_1 and M_2 are the reflective markers attached on the wheel,
- Y_m is the width of each marker,
- S_m denotes a diameter of circle (**201**) defined by rotating markers.

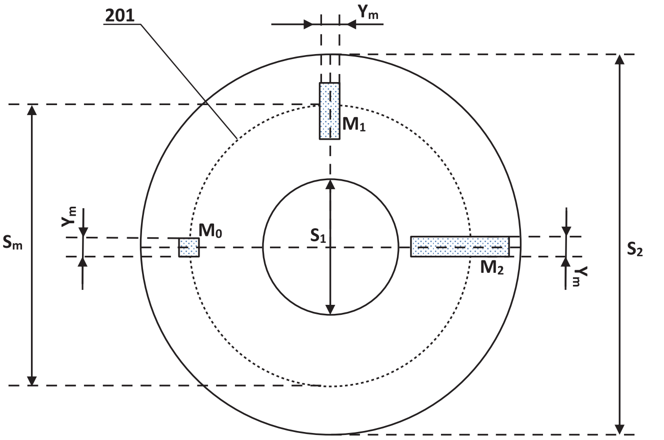

Fig. 2. Markers position on a wheel – example
Rys. 2. Przykładowe rozmieszczenie markerów odblaskowych na kole

The described system is designed to calculate the distance covered and the runner's current speed. Based on the arrangement of the sensor (7) relative to the marker (6), it can also detect the direction of movement. This is achieved by placing at least one marker on the driving wheel (2) (as illustrated in Fig. 2), where C_m represents the number of markers (e.g., reflective markers configured to reflect specific wavelengths, such as infrared light or a portion of the visible spectrum).

Additionally, a sensor (7) for detecting the marker and its movement direction is positioned near the driving wheel (2). This sensor is capable of detecting signals (e.g., specific wavelengths) emitted toward the markers and reflected back. The sensor can also be integrated with an emitter that generates these signals.

By knowing the diameter S_1 of the wheel (2) and the number of markers C_m positioned on it, the distance traveled by the working belt (5) can be calculated as one circumference O_{S1} of a circle with a diameter of S_1.

For instance, if $C_m = 1$ (meaning a single marker is placed on the wheel), then each detection of the marker indicates that the belt (5) moves by:

$$S_1\pi \tag{1}$$

When $C_m > 1$, it becomes possible to measure the distance traveled by the working belt (5) with greater precision than by using only O_{S1} (the circumference of the wheel). This is because the markers can be placed in a non-symmetrical arrangement. However, this requires knowing the distance between the markers and the diameter S_m of the circle on which the markers are positioned on the driving wheel (2), as illustrated in Fig. 2, item **201**. In such a case, the distance can be calculated as:

$$CO_{S1} + D, \tag{2}$$

where: C – the number of complete revolutions of the wheel (2) (or, equivalently, the number of detections of the markers C_m); D – the sum of the distances between markers counted during the last partial revolution.

Let O_m denote the circumference of the circle S_m (see Fig. 2, **201**). By knowing the distances between the markers along O_m, the angles between them can be calculated. This allows the determination of the angle by which the driving wheel (2) has rotated upon detecting a marker, which in turn indicates the percentage of the distance O_{S1} that the working belt (5) has traveled.

The system also calculates the current speed by measuring the time T_m during which the sensor detects a marker, as shown in Fig. 3.

By knowing the width Y_m of markers M_0, M_1, M_2, the value X_m can be calculated as a reference for a measurement along the circumference of a circle. Here, Y_m represents the physical width of a marker, while X_m corresponds to the length of the intersection between the marker and the circle's circumference.

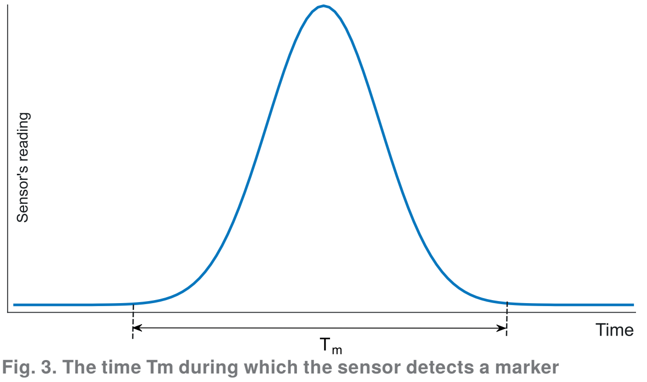

Fig. 3. The time Tm during which the sensor detects a marker
Rys. 3. Czas Tm w trakcie którego czujnik wykrywa marker

Given S_m (the circle's diameter) and Y_m, X_m can be determined, representing its dimension along the circumference where the marker is positioned. The marker is rectangular in shape, and knowing the circumference O_m and time T_m, the angular speed of the driving wheel (2) can also be calculated.

In other words, X_m represents a segment of a virtual circumference of a circle that intersects with the marker. As illustrated in Fig. 2, all markers M_0, M_1, and M_2 share the same width Y_m, while their other dimensions can be selected freely. A longer marker (e.g., M_2, being the longest) is preferable because it is easier to mount. However, even though using a longer marker can simplify the mounting process, the placement of the marker is not arbitrary.

The markers M_0, M_1, and M_2 are positioned so that their length aligns with the radius of the driving wheel (2).

For this purpose, the markers are preferably rectangular, as this ensures that a sensor measuring the circumference will always detect the same arc, regardless of the marker's placement along the radius. However, this condition is not fulfilled at the ends of the marker, where only the corners might be detected. Therefore, the longer the marker, the better—ideally extending the full length of the driving wheel's (2) radius—to ensure that the chosen circumference of the wheel intersects the full width of the marker. As a result, a circular shape is generally not preferred (though not entirely excluded) for such a marker, since different crossing points between a circle and the circumference would define different arcs.

It is evident that the speeds of both the driving wheel (2) and the driving shaft (1) are the same. By knowing O_{S1} and the speed, the distance traveled by the working belt (5) during time T_m can be calculated. This also allows for determining the speed of the working belt (5) at the moment the sensor detects the marker.

An relevant equations can be defined as follows:

$$V_b = \frac{\frac{x_m}{O_m} O_{S1}}{T_m} \tag{3}$$

That results in:

$$V_b = \frac{x_m S_1}{S_m T_m} \tag{4}$$

However, for this to function properly, S_m must be determined. As previously explained, this can be challenging in legacy systems where access to the driving wheel or driving shaft is limited. Furthermore, determining S_m requires accurate placement of the markers and precise measurement of the distance between them along the circumference. Additionally, the sensor must be positioned with great precision since the circumference S_m is defined by the relative positions of the sensor and the markers.

An error in determining the S_m diameter will accumulate and amplify at various stages of the calculation, leading to a significant error in the final result for the current speed. This issue is particularly pronounced with smaller S_m diameters, where errors tend to be more substantial. For example, a 1 mm error on an S_m of 100 mm results in a 1 % error in the current speed.

Finally, the need for high precision leads to longer installation times, which raises deployment costs. Therefore, an easy and automatic method for determining the diameter S_m and the relative positioning of the markers is highly advantageous, as it addresses these issues effectively.

The proposed solution involves only a simple installation of a sensor and at least one marker, without needing to specify the exact circumference (or radius). Any potential calcula-

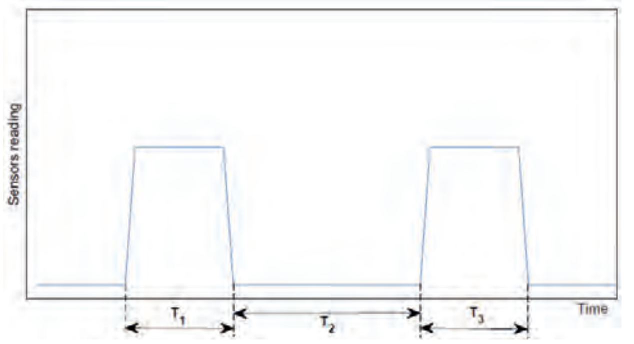

Fig. 4. The sensor data for a single marker includes measurements of the marker's presence times T1 and T3, as well as the intervals between marker detections T2
Rys. 4. Zmierzony czas odczytywania obecności markera T1 i T3 oraz czas między odczytami markerów T2

tion error is mitigated through a statistical measurement of the S_m diameter.

Figure 4 shows the readings from a sensor for a single marker, including the measured times of the marker's presence and the intervals between its detections.

Given the marker width Y_m and the times T_1, T_2, and T_3, the following calculations can be made:

- A distance traveled in time $T_1 + T_2$ or $T_2 + T_3$.
- The distance X_m (partial result), which represents the length of the arc formed by the marker's width Y_m along the circumference of the circle S_m (or the distance traveled between the start and end of the sensor reading).
- The angle α (partial result), which is the angle at the base of an isosceles triangle defined by the chord X_m as the base and two equal arms each measuring $\frac{1}{2}S_m$.
- The speed at the first detection of the marker is X_m/T_1, while at the second detection, it is X_m/T_2.

Therefore, the circumference O_m can be determined by multiplying the average speed (calculated from the two measurements) by the time T_2 between marker detections and then adding the marker width, as follows:

$$O_m = \frac{\frac{x_m}{T_1} + \frac{x_m}{T_3}}{2} T_2 + X_m \tag{5}$$

Thus, the diameter S_m can be determined by solving the given set of equations:

$$S_m = \frac{\frac{\frac{x_m}{T_1} + \frac{x_m}{T_3}}{2} T_2 + X_m}{\pi} \tag{6}$$

$$\sin\left(\frac{\alpha}{2}\right) = \frac{Y_m}{S_m} \tag{7}$$

$$X_m = \frac{\alpha S_m}{2} \tag{8}$$

for α given in radians.

This assumes that the speed changes in linear manner between the markers. By conducting multiple measurements, the average result will converge to the true value. For more than one marker, calculating S_m will involve solving the following equations:

$$A_{12} = \frac{\frac{x_m}{T_1} + \frac{x_m}{T_3}}{2} T_2 + X_m, \tag{9}$$

$$A_{23} = \frac{\frac{x_m}{T_3} + \frac{x_m}{T_5}}{2} T_4 + X_m, \tag{10}$$

$$A_{34} = \frac{\frac{x_m}{T_5} + \frac{x_m}{T_7}}{2} T_6 + X_m, \tag{11}$$

$$\vdots$$

$$A_{NM} = \frac{\frac{x_m}{T_{N-1}} + \frac{x_m}{T_M}}{2} T_N + X_m, \tag{12}$$

where A_{NM} represents the length of the arc on the circle with circumference S_m from marker N to marker M. The sum of all A values should equal S_m.

Figure 5 illustrates a diagram of the system according to the proposed approach. The system can be implemented using dedicated components or custom FPGA or ASIC circuits. It includes a data bus (5-01) connected to a memory unit (5-04). Additionally, other components are linked to the system bus (5-01), allowing them to be managed by a controller circuit (5-05).

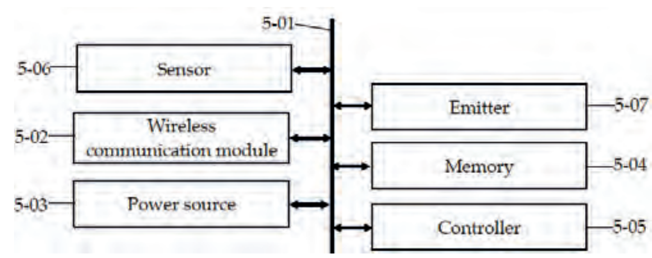

Fig. 5. The proposed system diagram
Rys. 5. Diagram zaproponowanego systemu

The memory unit (5-04) may store computer programs executed by the controller (5-05) to perform the method's steps. The system is powered by a battery (5-03) but can also be connected to mains power. Additionally, it is advisable to incorporate a wireless communication module (5-02) to facilitate the transfer of distance and speed data to other devices. This module can also be used for monitoring and configuring the system's status. The sensor (5-06) is designed to detect signals (e.g., specific wavelengths) emitted toward and reflected by the markers. It may also be integrated with an emitter (5-07) that produces such signals, such as visible light, infrared, or similar.

Figure 6 illustrates the method according to the proposed approach. The process begins with step (6-01), where a marker (M_0, M_1, M_2) with a specified width Y_m is acquired. Multiple markers may be used.

Next, in step (6-02), a circumference with a specified radius is selected for positioning the marker. The circumference can be associated with the center of the marker, where the marker's length matches the radius of the circumference, and its width is oriented perpendicularly to the radius.

Subsequently, in step (6-03), the markers are mounted on the selected circumference. In step (6-04), the sensor is positioned to detect the presence of the marker at a specific location. Typically, the sensor's field of view is limited to a section of the circumference, and it will detect the marker as it passes through this field of view.

In step (6-05), the wheel with the mounted marker (such as the driving wheel (2)) is rotated so that the sensor can detect

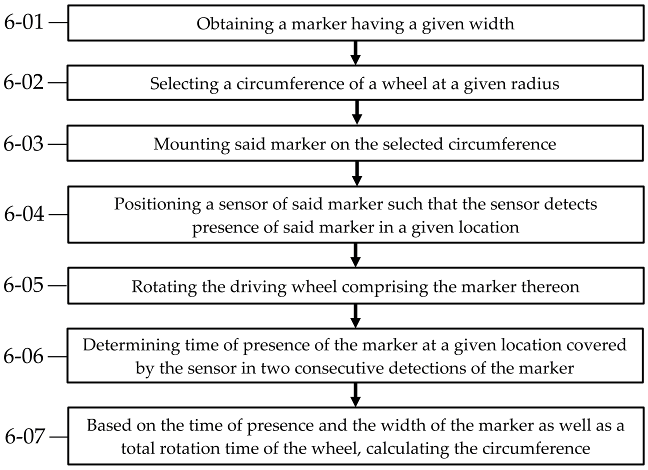

Fig. 6. The proposed method diagram
Rys. 6. Diagram zaproponowanej metody

the marker. Steps (6-01) through (6-05) are considered setup steps, while the subsequent steps are operational steps performed by the detection and measurement system.

Next, in step (6-06), the time during which the marker is present in the sensor's field of view is determined based on two consecutive detections, as illustrated by times T_1, T_2, and T_3 in Fig. 4. The region monitored by the sensor is known as its field of view.

In the final step (6-07), the circumference is determined by considering the duration of presence, the marker's width, and the overall wheel rotation time. With the circumference and the total rotation time, the speed can be computed, as detailed in the equations provided earlier.

3. Experimental tests

Experimental tests were conducted to evaluate the effectiveness of a proposed method for measuring the speed and travelled distance, which are the most significant from the user's perspective. A sensor, presented in Fig. 7, configured to detect signals emitted towards a marker and reflected by the marker, was positioned near the wheel to detect the direction of its movement (Fig. 8).

The motor-driven wheel constituted the propulsion component of the Matrix treadmill, presented in Fig. 9.

During the experiment, the readings on the treadmill's attached screen were compared with the measurements taken by the proposed sensor. The measurement accuracy was 0.01. Additionally, they were compared with the actual speed and travelled distance measured using the conventional formula:

$$V = \frac{S}{t}, \tag{13}$$

where V is a speed of a treadmill, S is a distance and t is time These calculations were performed with the same accuracy of 0.01.

For precise measurement of actual values, the length of the belt was measured and markers were placed on it. The length

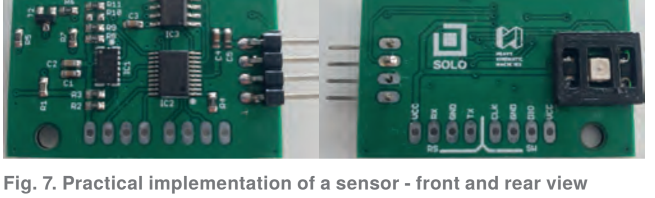

Fig. 7. Practical implementation of a sensor - front and rear view
Rys. 7. Praktyczne wykonanie czujnika – wygląd z przodu i z tyłu

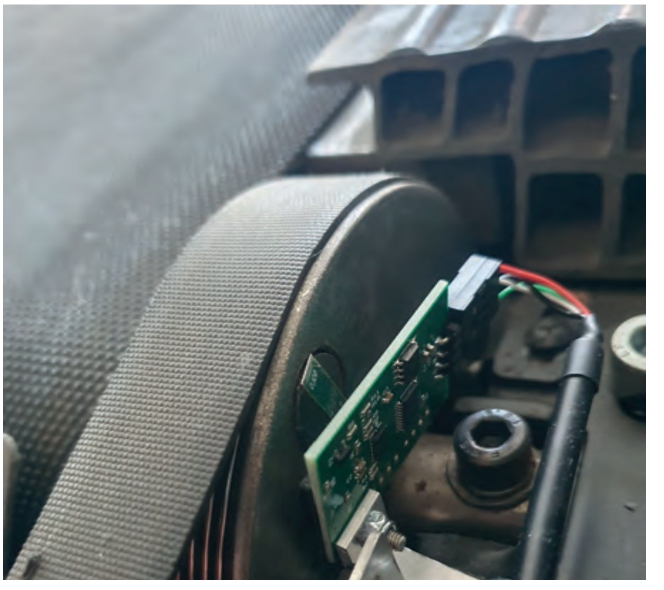

Fig. 8. Example placement of the sensor
Rys. 8. Przykładowe umieszczenie czujnika pomiarowego

Fig. 9. The Matrix company treadmill on which tests were conducted
Rys. 9. Bieżnia treningowa firmy Matrix, na której były wykonywane test praktyczne

of the belt was 3.297 m. Time was measured using a stopwatch. Note that this treadmill displays the first distance after covering 0.1 miles, which is also its maximum precision. In the case of proposed sensor, the value readings occur every second. The treadmill screen displays values in miles; therefore, the results have been converted into SI units. Table 1 presents the results of the actual speed measurement calculated using formula 13, as well as the values displayed on the treadmill screen and those read from the proposed sensor. It follows from these results that the values read from the sensor are closer to the actual values, which is better illustrated in Tab. 2, where measurement errors are shown in percentages.

The same results in a different form are presented in Fig. 10.

To measure the distance travelled, the treadmill was started at various speeds, and values were read at random moments. Readings displayed on the screen were compared with values read by the proposed sensor and measurements obtained according to the transformed formula 13. The measurement results have been presented in Tab. 3.

Table 4 presents difference between the real travelled distance and the distance indicated by the treadmill screen as well as the proposed sensor. It follows from it that also in the

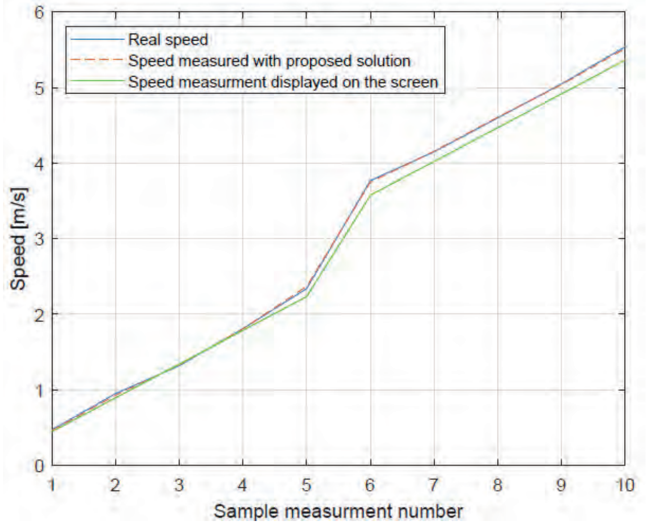

Fig. 10. Values of the speed given by the built-in sensor, by the sensor proposed in this paper, and the actual speed
Rys. 10. Prędkość zmierzona przy użyciu wbudowanego w bieżnię czujnika w porównaniu do prędkości zmierzonej przez czujnik zaproponowany w tym artykule oraz prędkość rzeczywista

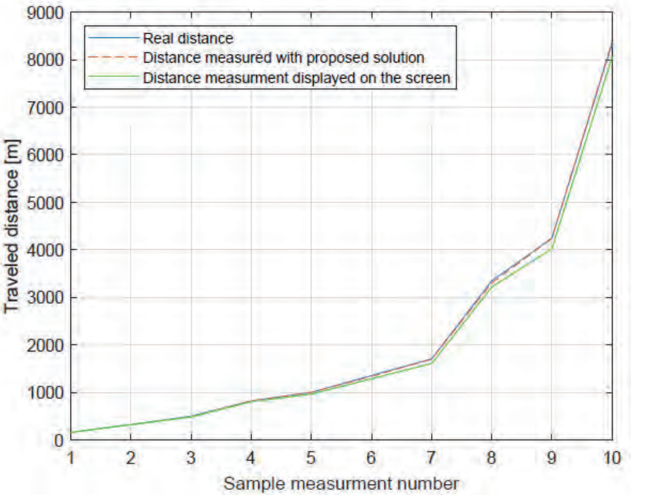

Fig. 11. Values of the travelled distance given by the built-in sensor, by the sensor proposed in this paper, and the actual speed
Rys. 11. Przebyta droga zmierzona przy użyciu wbudowanego w bieżnię czujnika w porównaniu do prędkości zmierzonej przez czujnik zaproponowany w tym artykule oraz prędkość rzeczywista

Table 1. The speed measured and displayed by the treadmill's screen, by the proposed sensor, and the actual measurement according to (13)
Tabela 1. Prędkość pokazywana na wyświetlaczu bieżni, prędkość zmierzona przy użyciu zaproponowanego czujnika i rzeczywista prędkość wyznaczona wzorem (13)

Sample measurement number	Treadmill speed displayed on the dedicated screen		Proposed solution speed read direct from the sensor [m/s]	Real measured speed calculated with (13) [m/s]
	[miles/h]	[m/s]		
1	1	0.45	0.46	0.47
2	2	0.89	0.92	0.95
3	3	1.34	1.32	1.32
4	4	1.79	1.80	1.81
5	5	2.24	2.36	2.34
6	8	3.58	3.74	3.77
7	9	4.03	4.15	4.15
8	10	4.47	4.60	4.60
9	11	4.92	5.03	5.05
10	12	5.37	5.51	5.54

Table 2. The difference between the actual speed and the speed indicated by the treadmill screen as well as the proposed sensor
Tabela 2. Różnica prędkości pokazywanej na wyświetlaczu bieżni, prędkości zmierzonej przy użyciu zaproponowanego czujnika i rzeczywistej prędkości

Sample measurement number	Difference between treadmill speed and proposed solution speed [%]	Difference between treadmill speed and real speed [%]	Difference between proposed solution speed and real speed [%]
1	-3.33	4.88	1.71
2	-3.84	5.88	2.27
3	0.88	-1.60	-0.70
4	-1.12	1.20	0.09
5	-6.00	4.47	-1.25
6	-4.81	5.13	0.57
7	-3.38	3.05	-0.22
8	-3.11	2.81	-0.20
9	-2.47	2.62	0.21
10	-2.87	3.16	0.39

Table 3. The travelled distance measured and displayed by the treadmill's screen, by the proposed sensor, and the actual measurement according to transformed (13)

Tabela 3. Przebyta odległość pokazywana na wyświetlaczu bieżni, zmierzona przy użyciu zaproponowanego czujnika oraz rzeczywista wyznaczona wzorem (13)

Treadmill speed displayed on the dedicated screen [miles/h]	Treadmill distance displayed on the dedicated screen		Proposed solution distance read direct from the sensor [m]	Real measured distance calculated with transformed 13 [m]
	[miles]	[m]		
1.0	0.1	160.93	161.93	162.34
1.1	0.2	321.86	322.39	325.47
1.3	0.3	482.80	489.92	499.34
1.5	0.5	804.67	825.93	821.93
1.6	0.6	965.60	1003.43	1001.37
1.8	0.8	1287.40	1335.23	1355.99
4.0	1.0	1609.34	1700.23	1705.29
8.0	2.0	3218.69	3301.04	3345.23
10.0	2.5	4023.36	4244.93	4245.95
12.0	5.0	8046.72	8380.25	8333.88

Table 4. The difference between the real travelled distance and the distance indicated by the treadmill screen as well as the proposed sensor

Tabela 4. Różnica przebytej odległości pokazywanej na wyświetlaczu bieżni. zmierzonej przy użyciu zaproponowanego czujnika i rzeczywistej odległości

Treadmill speed displayed on the dedicated screen [miles/h]	Difference between treadmill distance and proposed solution distance [%]	Difference between treadmill distance and real distance [%]	Difference between proposed solution distance and real distance [%]
1.0	-0.62	0.86	0.25
1.1	-0.16	1.10	0.94
1.3	-1.47	3.31	1.88
1.5	-2.64	2.10	-0.48
1.6	-3.92	3.57	-0.20
1.8	-3.71	5.05	1.53
4.0	-5.65	5.62	0.29
8.0	-2.56	3.78	1.32
10.0	-5.51	5.24	0.02
12.0	-4.15	3.44	-0.55

case of measuring the distance travelled, the proposed sensor performs better, yielding a smaller measurement error than the treadmill's built-in system, which is shown in Fig. 11.

The tests demonstrated that the sensor was able to accurately detect the speed of the treadmill, even at high speeds, and regardless of the position of the marker placed on moving wheel.

The results obtained from the tests were consistent, with negligible error margins, even when taking into account a small error in measuring the real values.

Furthermore, the sensor was able to perform measurements in a variety of scenarios, demonstrating the versatility of this method.

Overall, the tests confirmed the reliability and effectiveness of the proposed method for observing movement of a driving wheel and deriving speed and distance travelled through these measurements. This research is expected to contribute to the development of more accurate and reliable measurement techniques in various industries.

4. Conclusions

The study presents a novel, non-contact method for measuring the rotational speed of a wheel without prior knowledge of its dimensions. This approach addresses significant challenges faced by traditional systems, particularly in applications where accessing or accurately measuring the wheel's dimensions is impractical. By employing a sensor and reflective markers, the proposed method enables precise determination of speed and distance, as confirmed through experiments conducted on a treadmill.

The experimental results demonstrate that the proposed method yields highly accurate measurements, outperforming the built-in treadmill system in both speed and distance accuracy. The measured values closely align with actual values, showcasing negligible error margins even under varying conditions. Furthermore, the versatility of the method was validated by its ability to adapt to different speeds and marker positions.

This method is particularly beneficial for retrofitting legacy systems, as it simplifies the installation process and eliminates the need for precise knowledge of wheel dimensions. Beyond treadmills, the method holds potential for broader industrial applications, such as monitoring turbine speed in power plants, controlling machinery in automated processes, and measuring performance in fluid transport systems.

Overall, the proposed system provides a cost-effective, reliable, and versatile solution for rotational speed measurement, making it a valuable contribution to both the fitness equipment industry and other industrial domains. Future research could explore further optimization of the system and its application in more diverse scenarios.

Acknowledgements

This research was funded by The National Centre for Research and Development in Poland. grant number POIR.01.01.01-00-0345/22-00.

References

1. Whitman A., Clayton G., Ashrafiuon H., *Prediction of wheel slipping limits for mobile robots*, "Journal of Dynamic Systems, Measurement, and Control", Vol. 141, No. 4, 2019, DOI: 10.1115/1.4041664.
2. Szolc T., *Selected problems of rotating machinery dynamics*, "Bulletin of the Polish Academy of Sciences Technical Sciences", Vol. 71, No. 6, 2023, DOI: 10.24425/bpasts.2023.148442.
3. Qiu H., Wei Y., Zhao X.F., Yang C., Yi R., *Research on the influence of rotational speed on the performance of high-speed permanent-magnet generator*, "Archives of Electrical Engineering", Vol. 68, No. 1, 2019, 77–90, DOI: 10.24425/aee.2019.125981.
4. Foster D.A., *Developments in wheel speed sensing*, [In:] SAE International Congress and Exposition, SAE International, 1988, DOI: 10.4271/880325.
5. Hainz S., de la Torre E., Güttinger J., *Comparison of magnetic field sensor technologies for the use in wheel speed sensors*, [In:] 2019 IEEE International Conference on Industrial Technology (ICIT), IEEE, 2019, 727–731, DOI: 10.1109/ICIT.2019.8755074.
6. Gao J., Petovello M., Cannon M., *Development of Precise GPS/INS/Wheel Speed Sensor/Yaw Rate Sensor Integrated Vehicular Positioning System*, Proceedings of the 2006 National Technical Meeting of The Institute of Navigation, 2006, 780–792.
7. Berntorp K., *Joint Wheel-Slip and Vehicle-Motion Estimation Based on Inertial, GPS, and Wheel-Speed Sensors*, "IEEE Transactions on Control Systems Technology", Vol. 24, No. 3, 2015, 1020–1027, DOI: 10.1109/TCST.2015.2470636.
8. Liu Z., Liu X., Li K., *Deeper exercise monitoring for smart gym using fused RFID and CV data*, [In:] IEEE INFOCOM 2020 – IEEE Conference on Computer Communications. IEEE, 2020, 11–19, DOI: 10.1109/INFOCOM41043.2020.9155360.
9. Luzar M., Czajkowski A., Kasperowicz R., Rot M., Semegen M., Korbicz J., *Sensor-based weightlifting workout assisting system design and its practical implementation*, "Journal of Sensors", 2019, DOI: 10.1155/2019/1787351.
10. Li G.-Y., Li J., Li Z.-J., Zhang Y.-P., Zhang X., Wang Z.-J., Han W.-P., Sun B., Long Y.-Z., Zhang H.-D., *Hierarchical PVDF-HFP/ZnO composite nanofiber – based highly sensitive piezoelectric sensor for wireless workout monitoring*, "Advanced Composites and Hybrid Materials", Vol. 5, No. 2, 2022, 766–775, DOI: 10.1007/s42114-021-00331-z.
11. Joseph R., Ayyappan M., Shetty T., Gaonkar G., Nagpal A., *BeFit – a real-time workout analyzer*, [In:] Sentimental Analysis and Deep Learning: Proceedings of ICSADL, Springer, 2022, 303–318, DOI: 10.1007/978-981-16-5157-1_24.
12. Hardy S., Dutz T., Wiemeyer J., Göbel S., Steinmetz R., *Framework for personalized and adaptive game-based training programs in health sport*, "Multimedia Tools and Applications", Vol. 74, 2015, 5289–5311, DOI: 10.1007/s11042-014-2009-z.
13. Thompson W.R., *Worldwide survey of fitness trends for 2019*, "ACSM's Health & Fitness Journal", Vol. 22, No. 6, 2018, 10–17, DOI: 10.1249/FIT.0000000000000438.
14. Semegen M., Rot M., Ostrowski K., Kasperowicz R., *System and method for measuring speed*, International Patent no: WO2022089764A1.
15. Luzar M., Witczak M., *Fault-tolerant control and diagnosis for LPV system with H-infinity virtual sensor*, 3rd International Conference of Control and Fault-Tolerant Systems (SysTol), 2016, 825-830, DOI: 10.1109/SYSTOL.2016.7739849.

System i bezkontaktowa metoda mierzenia prędkości koła: przykład z wykorzystaniem bieżni do ćwiczeń

Streszczenie: W artykule zaproponowano innowacyjne podejście do mierzenia prędkości koła. W tym celu zaproponowana metoda jest w stanie automatycznie wyznaczyć wymiary koła takie jak promień, średnica i obwód. Dlatego to podejście znajduje zastosowanie tam, gdzie zmierzenie tych fizycznych parametrów jest trudne lub niemożliwe. W celu weryfikacji efektywności zaproponowanego rozwiązania, przeprowadzono praktyczny eksperyment z wykorzystaniem bieżni treningowej, której taśma jest przesuwana przy pomocy kół pasowych. Oryginalność przedstawionej metody potwierdzona jest przyznaniem patentu o numerze WO2022089764A1.

Słowa kluczowe: czujnik optoelektroniczny, pomiary, akwizycja danych

Marcel Luzar, PhD Eng.
m.luzar@pans.glogow.pl
ORCID: 0000-0002-3491-4113

He was born in 1985. Upon obtaining his MSc degree in computer science in 2009, he started working at the University of Zielona Góra, Poland, at the Institute of Control & Computation Engineering. In 2016, he obtained a PhD degree in automatic control and robotics. Luzar was an Erasmus exchange student at the Polytechnic University of Catalonia and a recipient of a grant from the National Science Centre in Poland for his research work, which includes fault-tolerant control and artificial intelligence. He has published more than 30 papers in international journals, book chapters, and conference proceedings. His teaching interests include PLC programming, SCADA systems, and intelligent control methods. Luzar enjoys playing sports (especially table tennis) and motorcycling.

Kacper Ostrowski, MSc Eng.
kacper.ostrowski@heavykinematic.com
ORCID: 0009-0004-9004-7730

He was born in 1990. He obtained his MSc degree in computer science in 2014 at the University of Zielona Góra. He has been involved in several R&D projects in fields such as image, video, and point cloud processing, IMU-based systems, optical-based sensing, and more. He is the inventor of 6 patents and patent applications.

Rafał Kasperowicz, PhD Eng.
rafal.kasperowicz@heavykinematic.com
ORCID: 0000-0001-7787-5006

He was born in 1978. He received his MSc degree in Management in 2002 and his PhD degree in Economics in 2006, both at the Poznań University of Economics and Business. His research areas are entrepreneurship, business cycle, economic growth, and energy. He has published more than 30 papers in international journals, book chapters, and conference proceedings. His teaching interests include microeconomics and entrepreneurship. He also has practical experience as a business developer and member of supervisory boards.

Mateusz Semegen, MSc Eng.
mateusz.semegen@heavykinematic.com
ORCID: 0009-0008-8857-6843

He was born in 1988. He obtained his MSc degree in computer science in 2013 at the University of Zielona Góra. He has many years of experience in creating and designing computer systems. He specializes in embedded systems based on ARM processors. In his free time, he plays drums, reads books, and travels.

Prof. Józef Korbicz, DSc PhD, full member of the Polish Academy of Sciences
j.korbicz@issi.uz.zgora.pl
ORCID: 0000-0001-8688-3497

He has been a full-rank professor of automatic control at the University of Zielona Góra, Poland, since 1994. In 2007 he was elected a corresponding member of the Polish Academy of Sciences (PAS). His current research interests include fault detection and isolation (FDI), control theory, and computational intelligence. He has published more than 370 scientific publications, authored or co-authored 8 books, and co-edited 7 books. This was confirmed by his appointment to prestigious positions such as IPC chairman of the IFAC Symposium SAFEPROCESS held in Beijing, China (2006), and NOC chairman of the NOC in Warsaw, Poland (2018). Together with Prof. J.M. Kościelny, he founded the Polish SAFEPROCESS conferences on Diagnostics of Processes and Systems (DPS), organized every two years (the 13th edition took place in 2017). He is currently the chair of the Committee on Automatic Control and Robotics of the PAS, a senior member of IEEE, and a member of the IFAC SAFEPROCESS TC.